

Thermal Analysis of a Transport Refrigeration Power Pack Unit Using a Coupled 1D/3D Simulation Approach

A. Kospach, A. Mladek, M. Waltenberger, F. Schilling

Abstract—In this work, a coupled 1D/3D simulation approach for thermal protection and optimization of a trailer refrigeration power pack unit was developed. With the developed 1D/3D simulation approach thermal critical scenarios, such as summer, high-load scenarios are investigated. The 1D thermal model was built up consisting of the thermal network, which includes different point masses and associated heat transfers, the coolant and oil circuits, as well as the fan unit. The 3D computational fluid dynamics (CFD) model was developed to model the air flow through the power pack unit considering convective heat transfer effects. In the 1D thermal model the temperatures of the individual point masses were calculated, which served as input variables for the 3D CFD model. For the calculation of the point mass temperatures in the 1D thermal model, the convective heat transfer rates from the 3D CFD model were required as input variables. These two variables (point mass temperatures and convective heat transfer rates) were the main couple variables for the coupled 1D/3D simulation model. The coupled 1D/3D model was validated with measurements under normal operating conditions. Coupled simulations for summer high-load case were than performed and compared with a reference case under normal operation conditions. Hot temperature regions and components could be identified. Due to the detailed information about the flow field, temperatures and heat fluxes, it was possible to directly derive improvement suggestions for the cooling design of the transport refrigeration power pack unit.

Keywords—Coupled thermal simulation, thermal analysis, transport refrigeration unit, 3D computational fluid dynamics, 1D thermal modelling, thermal management systems.

I. INTRODUCTION

THE road transport sector plays an important role in achieving climate goals. Worldwide, in 2014 transport as a whole was responsible for 23% of total CO₂ emissions from fuel combustion and road transport was responsible for 20% [1]. Trucks carry 73.1% of all freight transported over land in the European Union [2]. Although trucks account for less than 2% of vehicles in Europe, they were responsible for 23% of CO₂ emissions from road transport in 2019. And their emissions are increasing rapidly (+9% between 2014 and 2019) [3]. Transport refrigeration units (TRU) are used for temperature control of products, which are transported in various trucks, semi-trailers, and vans. Improving the efficiency and functional safety of such TRUs helps achieve the climate goals in the road freight

Alexander Kospach is with Virtual Vehicle Research GmbH, Inffeldgasse 21a, 8010 Graz, Austria (phone: +433168739055, e-mail: alexander.kospach@v2c2.at).

Alexander Mladek and Michael Waltenberger are with Virtual Vehicle Research GmbH, Inffeldgasse 21a, 8010 Graz, Austria (e-mail:

transport sector.

A transport semi-trailer refrigeration unit was investigated. The investigated TRU unit has three different modules. Each module consists of one evaporation path and one condensation path. The power supply and control module are in the power pack unit. In the power pack unit, the space is very limited, see Fig. 1. Different parts are packed extremely dense. Because of this dense packaging in the power pack unit, thermal management plays an important role. Experimental thermal protection analysis was done for selected operating points. The experiments can address some points, like questions of high surface component temperatures. The number of experiments is limited in the product development process because of the high costs and duration of one experiment. Especially important thermal critical scenarios, like hot air temperature outside, cannot be addressed experimentally for a tight cost and time schedule in the product development process. Simulations can overcome these drawbacks. Simulations provide information that is not experimentally accessible and complete or replace expensive experimental studies. For example, questions regarding critical temperature areas, so called hot spots, and warm air recirculation phenomena can only be addressed by simulation. Avoiding hot spots in the power pack unit is essential for functional safety. If these hot spots occur in thermal critical scenarios can also be verified by simulation.



Fig. 1 Transport refrigeration power pack unit for thermal analysis

alexander.mldadek@v2c2.at, michael.waltenberger@v2c2.at).

Florian Schilling is with Liebherr-Transportation Systems GmbH & Co KG, Liebherrstrasse 1, A-2100 Korneuburg, Austria, (e-mail: Florian.Schilling@liebherr.com).

In the past, especially for the engine compartment flow, 3D-CFD simulation methods were developed to avoid the critical temperatures and warm air recirculation phenomena [6]-[8]. In the field of road freight transport with temperature regulated freight, thermal numerical investigations within a refrigerated trailer were carried out, see [4] and [5]. To be able to evaluate the thermal characteristics of a transport refrigeration power pack unit a thermal network of the investigated components and coolant/oil circuit must also be considered. 1D thermal models are used as modelling approaches to model such systems [12], [13]. A detailed analysis of the thermal characteristics of a transport refrigeration power pack is therefore only possible with a coupled 1D/3D simulation approach. Coupled 1D/3D simulation approaches were developed for different vehicle thermal management systems but not for the thermal analysis of a transport refrigeration power pack unit [9]-[11]. This was the motivation to build up a coupled simulation approach for a transport refrigeration power pack unit to be able to investigate thermal characteristics during the development design phase. The simulation approach was used for the parking case. The parking case is defined as trailer with refrigeration unit but without the truck in parking position. This case was chosen first because in total the trailer refrigeration unit configuration is most of the time in this state.

In the next section the coupled simulation approach is

discussed in more detail.

II. COUPLED SIMULATION APPROACH

A. Coupled 1D/3D Thermal Model

In Fig. 2, the coupled 1D/3D model with the 1D thermal model block and the 3D-CFD model block is shown. 1D thermal model block provides the surface temperatures for the 3D-CFD model block. The 3D-CFD model block provides the convective heat fluxes for the defined warm components as boundary condition for the 1D thermal model block. Nine components were defined, which were coupled namely gear box, cylinder head, crankcase, oil pan, e-box, exhaust manifold, exhaust gas system, battery, and generator. The other components were modelled as adiabatic. The coupled simulation software was Model.Connect® from AVL. A coupling interface for OpenFOAM® was implemented as well to be able to couple the 3D model with the 1D model. The coupled values, as in Fig. 2, do not need to be exchanged every time step and a suitable coupling method for this application has been selected. The transient 1D thermal model was started for a certain time without coupling. At a certain point in time t_{offset} , coupling between the 1D and 3D models took place. However, a smaller time step was chosen for the 1D model than for the 3D model.

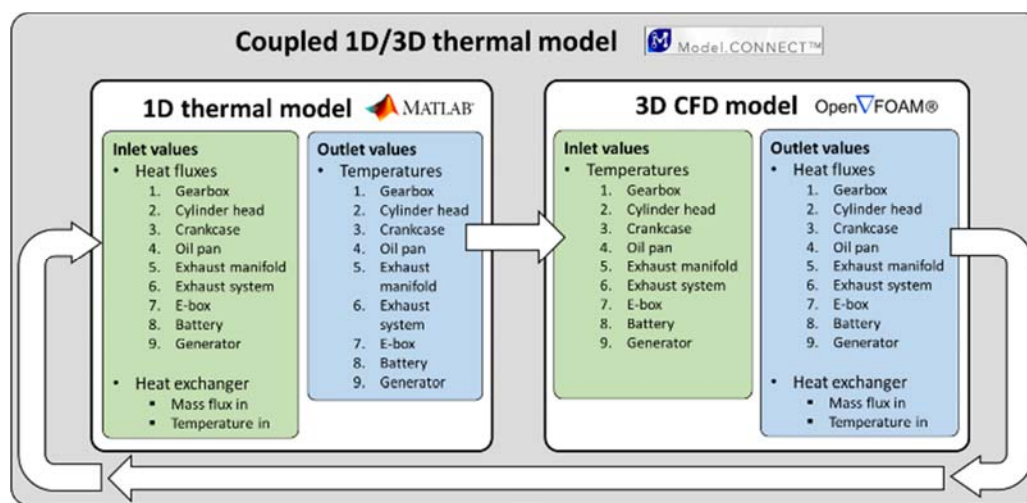


Fig. 1 Coupled 1D/3D model with the 1D thermal model block and the 3D CFD model block including the input and output values

B. 1D Thermal Model

The 1D thermal model consists of the thermal network, which includes nine point masses and their associated heat transfers, the coolant and oil circuits, the fan unit and coupled convective heat fluxes, see Fig. 3.

The thermal network with its nine point masses is described with its positions inside the power pack unit in detail in Fig. 4. Heat conduction between the point masses was considered in the thermal network, if necessary. In addition, the connections to the oil and cooling circuits for the different point masses are shown. For example, the point mass 3 crankcase has a connection to the oil and cooling circuit. For each point mass

there is a convective exchange with its surrounding.

Radiation was also considered as an additional heat quantity for each point mass in the thermal network modelling. The coolant circuit was modelled from the components, coolant pump, valves, cylinder head thermal bridge, crankcase thermal bridge, pipes, thermostat, and heat exchanger. The oil circuit was modelled from the same components as the coolant circuit. The fluid properties of oil were selected instead of the coolant fluid properties for the oil circuit. The fan was also modelled using a pressure loss polynomial. The pressure drop polynomial was created as a function of fan speed, air mass flow and air temperature.

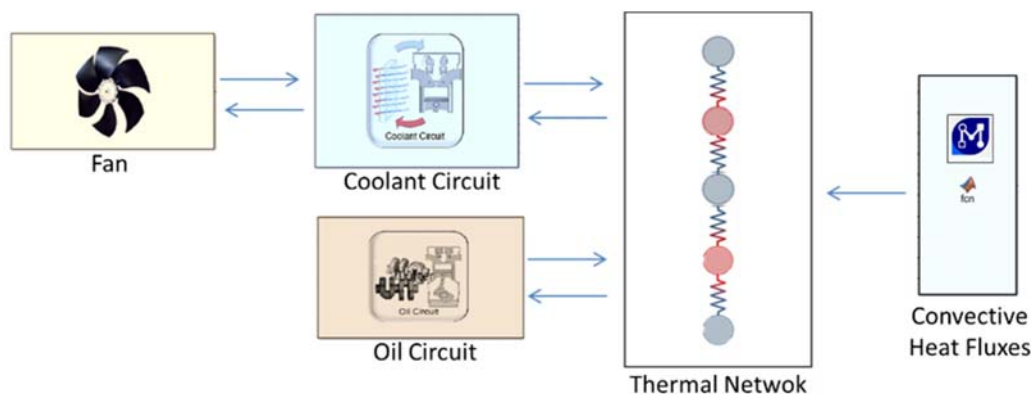


Fig. 3 1D thermal model of the trailer refrigeration power pack unit

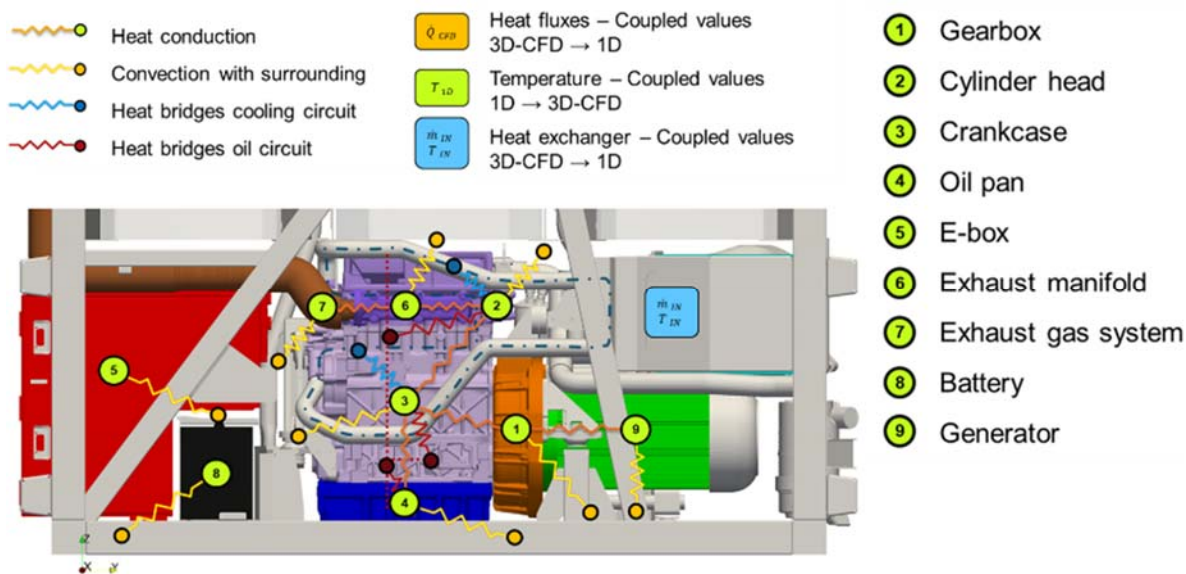


Fig. 4 1D thermal network model and positions of the nine point masses inside the power pack unit

Based on a consumption map, efficiency map and generator load point, an efficiency of the engine is calculated. Depending on the efficiency, a share for the waste heat and frictional power is then calculated. This distribution is used to derive the heat fluxes, which are used as input variables for the exhaust manifold, exhaust gas system, cylinder head and crankcase.

C. 3D-CFD Model

The 3D-CFD model will be described in two parts. First the geometry and the meshing will be explained in detail followed by the simulation approaches and settings.

The CAD geometry was meshed using the commercial pre-processor tool ANSA© by Beta CAE Systems. A watertight geometry was created by closing all small gaps. Some changes were done in the 3D-CFD geometry compared to the original geometry. The fan grill of the power pack unit was omitted to reduce the number of computational cells. Because just the power pack unit was considered, the openings of the condenser and evaporator paths were closed. The 3D-CFD geometry of TRU can be seen in Fig. 5. The cover of the TRU is shown transparent, and the power pack unit can be seen. A virtual test chamber was created for the 3D-CFD model. The trailer

refrigeration unit was placed on a simplified trailer model. The dimensions of the virtual wind tunnel were $\Delta x = 22.4$ m, $\Delta y = 20.48$ m and $\Delta z = 13.44$ m. The trailer refrigeration unit had the dimensions $\Delta x = 3.0$ m, $\Delta y = 2.5$ m and $\Delta z = 4.0$ m.

Meshing of the geometry was done with the routines BlockMesh and SnappyHexMesh from OpenFOAM©. A hex dominant volume mesh was created. The standard cell size for the geometry parts was around 2.5 mm to reach the criteria of near wall modelling. Certain components like the fan or the generator were meshed even with a smaller cell size. In total the number of cells was around 21.3 million.

The steady-state Reynolds-averaged Navier–Stokes (RANS) equations were solved for a compressible single-fluid flow. The numerical method used for solving the RANS equation is the finite volume method [15]. The turbulence k- ω -SST model was used and has proven to be suitable for such kind of heat transfer problems [16]. The density was determined by the state equation of an incompressible ideal gas with a fixed reference pressure. The specific heat capacity is assumed to be constant. The viscosity is described by a Sutherland model as a function of the temperature [17]. The energy equation was solved in the

formulation of the sensitive enthalpy. Radiation was not considered in the 3D-CFD model but was considered in the 1D thermal model. The modelling of the heat exchangers was done with a porosity model. The Darcy-Forchheimer porosity model was used [14]. The Darcy-Forchheimer coefficients were determined from test bench measurements and were set in local x direction. The porosity values in local y- and z-direction were set to a thousandfold of the porosity value of the x direction. No flow in y- and z-direction occurred inside the heat exchanger. The heat exchanger is located behind the fan. The fan blows hot air from the inside of the power pack unit to the outside ambient. The fan was modelled with an MRF (Multiple Reference Frame) approach which is widely used for modelling rotating components in steady state analysis [18]. The fan at the generator was not modelled directly using the MRF approach. Instead, a laminar inflow boundary condition around the generator blades was assumed. Based on this defined mass flow, a volume flow boundary condition for the outflow was defined. The laminar inflow velocity was specified from measurements.

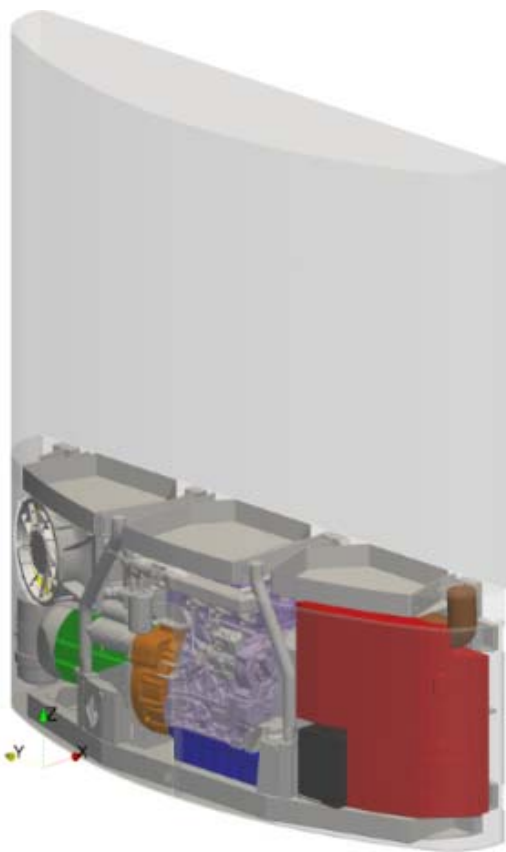


Fig. 5 TRU for the 3D-CFD model; the cover of the TRU is shown transparent

III. RESULTS

Two cases were investigated in detail for the thermal analysis of a trailer refrigeration power pack unit. First a reference case was examined for validation, calibration, and thermal analysis. Secondly, a summer high-load case was investigated for

thermal protection analysis. The coupled simulations were performed on different computers. The 3D-CFD simulations were performed on a cluster with 16 computational cores. The coupled simulation and the 1D thermal simulation were performed on a workstation with a single core. The results were analysed to determine critical thermal conditions. The 3D-CFD simulation accounted for all the simulation time. The simulations were run until the surface temperatures of the point masses reached a steady state.

A. Reference Case

The reference case was used as a validation case for the coupled simulation model. Measurements of the reference case were carried out. For the point masses cylinder head, crankcase, oil pan, e-box, exhaust manifold, battery and generator measured data of the surface temperature were available. The ambient temperature was 41 °C and this was the initial temperature for all point masses. No surface temperature measurement data were available for the point masses gearbox, crankcase, exhaust gas system. Furthermore, thermographic measurements were carried out for the exhaust after treatment to check for possible errors. For the coupled simulation, different time step sizes were used for the individual blocks. For the 3D-CFD simulation a time step size of 0.5 s was chosen for the coupling and for the 1D simulation a time step size of 0.1 s was chosen. The coupling time step size was chosen the same as the time step size of the 3D-CFD simulation. Up to time 1000 s, the 1D simulation ran alone. From time 1000 s, the 3D-CFD simulation was added, and full coupling began. This coupling strategy was used to reduce the simulation duration. The coupled simulation was calculated up to the final time 4000 s. From the time 3500 s, no noticeable changes in the temperatures and heat fluxes of the point masses can be observed. As result for the heat fluxes and temperatures at the point masses averaged values over 500 s were taken. The highest temperatures can be observed at the exhaust system and the manifold, see Fig. 6. The maximum heat flow is found at the generator with almost 1 kW. The lowest heat flows and temperatures are found at the battery, since in the coupled model can only be heated by the ambient air.

Temperature comparison

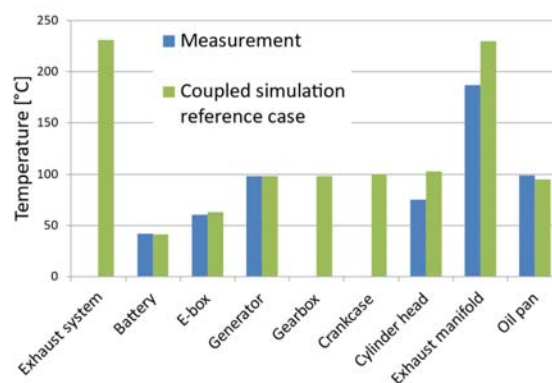


Fig. 6 Temperatures for the measurement and the coupled simulation reference case in comparison

Fig. 6 shows the temperatures for the measurement and the coupled simulation as a bar chart. For the measurement, there are no representative measured values for the point masses exhaust system, gearbox and crankcase. For the point masses battery, e-box, generator and oil pan, the relative error is below 5%. A clear deviation can be observed for the point masses cylinder head and exhaust manifold. For both point masses, the values of the coupled simulation are higher than in the measurements. The measuring point cylinder head for the measurement was applied at the suction side. An averaged head temperature should therefore be higher than the specified measured value. This minimizes the error of the coupled simulation to the measurement and provides an explanation for the deviation. The deviations of the simulation result of the point mass exhaust manifold to the measurement can be explained by the sensitivity to measurement point position and additional measurements are required to justify this assumption.

Furthermore, in a post-processing step, cuts were made through the power pack unit and evaluated for the field variables pressure, temperature, velocity, and turbulent kinetic energy. The individual cutting planes are shown in Fig. 7. Z- and y-cuts were made through the power pack unit region.

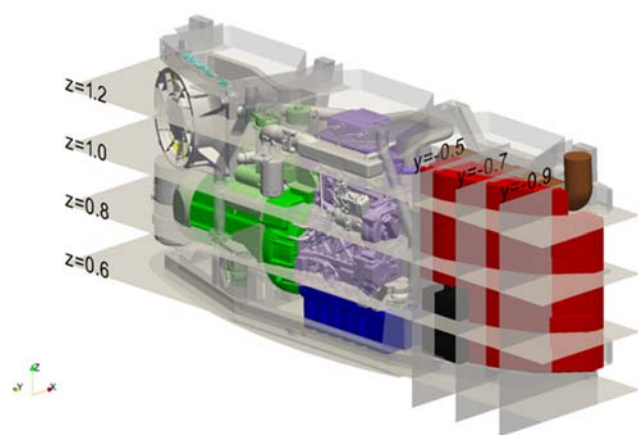


Fig. 7 Representation of the cutting planes through the power pack unit

In Fig. 8 the cutting planes at positions $z = 0.6$, $z = 0.8$ and $z = 1.0$ are shown for the temperature and the magnitude of the velocity fields. For the cutting planes $y = -0.5$ and $y = -0.9$ the temperature field is shown. Increased temperatures can be seen on the generator, combustion engine and exhaust system components. From the velocity distribution, a substantial part of the intake air is taken directly below the fan. The cooling effect of the convective heat transport could be optimized by appropriate simple measures, e.g. air baffles. Near the e-box and exhaust system, there is strong local heating. The velocities are relatively low to be able to transport the heat away, which leads to heating, see temperature diagrams for $y = -0.5$ and $y = -0.9$ in Fig. 8. The intake air entering the power pack unit is in the range of the ambient temperature, see cutting plane $z = 0.6$ for the temperature distribution in Fig. 8. Thus, there is no strong recirculation effect of the warm discharged air back into the power pack unit.

B. Summer High-Load Case

The validated coupled simulation model was used to calculate a summer high-load case for thermal analysis and protection. The ambient temperature was increased to $48\text{ }^{\circ}\text{C}$. The load point at the generator was increased from 13.4 kW to 18.4 kW . The same time step sizes were used for the summer high-load case as for the reference case. Again, coupling between 1D and 3D-CFD was not performed until time 1000 s . The initial condition for each point mass was again assumed to be ambient temperature. The coupled simulation was calculated up to the final time 6000 s . From the time 3500 s , no noticeable changes in the temperatures and heat fluxes of the point masses can be observed. Average values over 500 s were again taken for the heat flows and temperatures at the point masses. The highest temperatures can again be observed at the exhaust system and the manifold. The maximum heat flux is again found at the generator with 1.2 kW . The lowest heat fluxes and temperatures are found at the battery, since in the coupled model it can only be heated by the ambient air.

Fig. 9 shows the temperatures of the point masses for the measurement, coupled simulation reference case, and coupled simulation summer high-load case. Clearly all point mass temperatures are higher in the summer high-load case than for the coupled simulation reference case. The largest absolute temperature differences are found for the point masses exhaust system and exhaust manifold. The exhaust system and manifold have warmed by $77\text{ }^{\circ}\text{C}$ in the summer high-load case compared to the reference case. The e-box warmed by $30\text{ }^{\circ}\text{C}$. The relative change in temperatures was around 15% for the battery and e-box. For all other point masses, the relative change in temperature was about 30% compared to the reference case.

In addition, the convective heat fluxes of the coupled simulation reference and summer high-load case were compared. The strongest absolute increase of the heat flux can be observed at the generator. The increase is close to 300 W . The largest relative increase is observed at the point mass exhaust system. A relative increase of 41% can be recorded. The heat flux at the e-box is almost identical in the two coupled simulations. The fact that the heat fluxes at the e-box are constant points to possible improvement potentials regarding convective air cooling.

Fig. 11 shows the cut plots at positions $z = 0.6$, $z = 0.8$ and $z = 1.0$ for the temperature and magnitude of velocity fields. For the cut plots $y = -0.5$ and $y = -0.9$, the temperature field is shown. Again, increased temperatures can be observed at the generator, combustion engine and exhaust system components. It can be seen from the velocity distribution that a significant part of the intake air is drawn in directly below the fan again. Near the e-box, there is again strong local heating near the exhaust system. The velocities are relatively low to be able to transport the heat away, which leads to heating, see temperature plots for $y = -0.5$ and $y = -0.9$. The sucked air entering the power pack unit is again in the range of the ambient temperature, see cutting plane $z = 0.6$ for the temperature distribution. Thus, there is no strong recirculation effect of the warm discharged air back into the power pack unit. Velocity and temperature characteristics of the coupled simulation summer high load case

are similar to the reference case. This means that hot or high velocity regions are the same for both coupled simulations.

Larger differences can only be seen at the cylinder head.

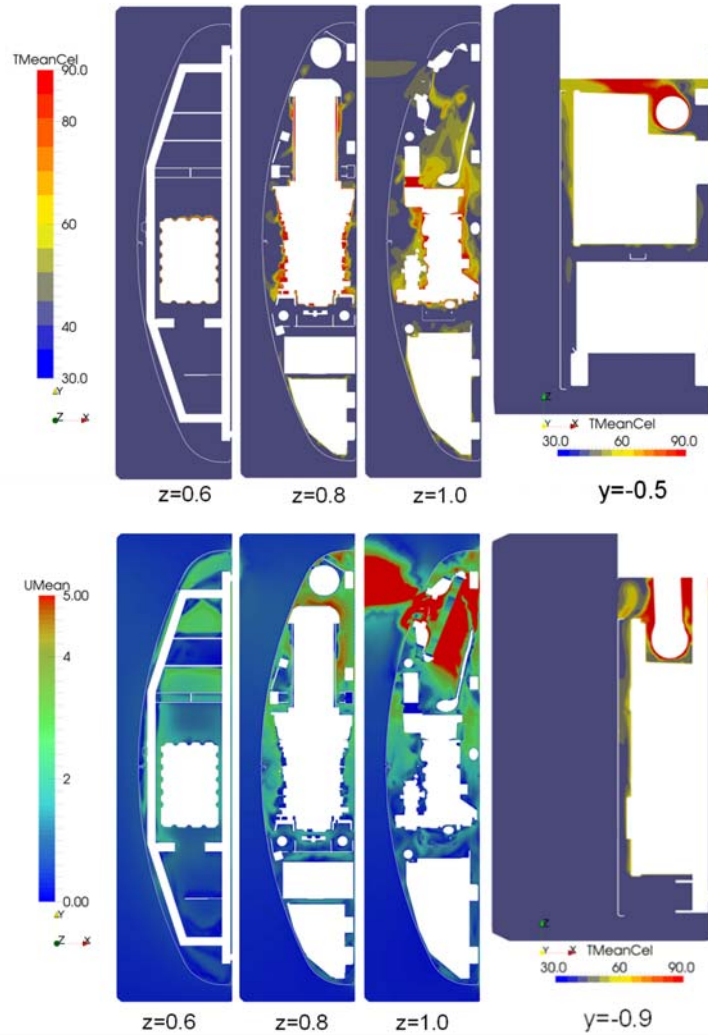


Fig. 8 Cut plots for the reference case at positions $z = 0.6$, $z = 0.8$ and $z = 1.0$ for the temperature and velocity magnitude fields; for the cut planes $y = -0.5$ and $y = -0.9$ the temperature field is shown

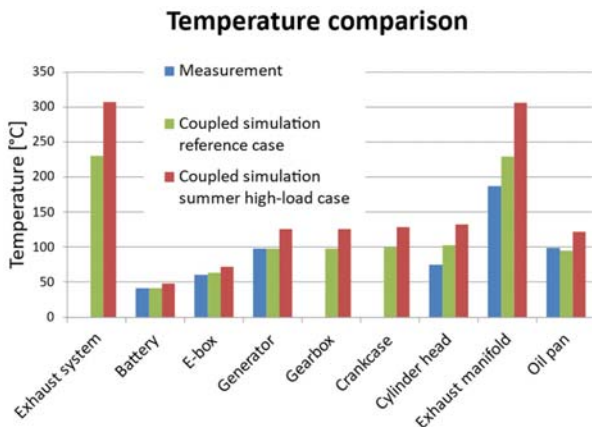


Fig. 9 Column chart of temperatures for the measurement, coupled simulation reference case and the coupled simulation summer high-load case in comparison

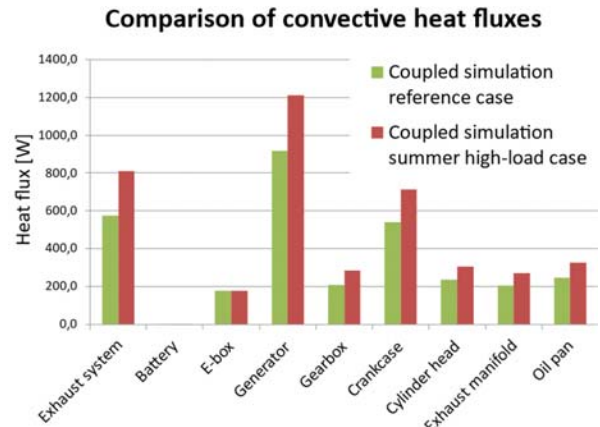


Fig. 10 Column plot of the heat fluxes of the coupled simulation reference case and the coupled simulation summer high-load case in comparison

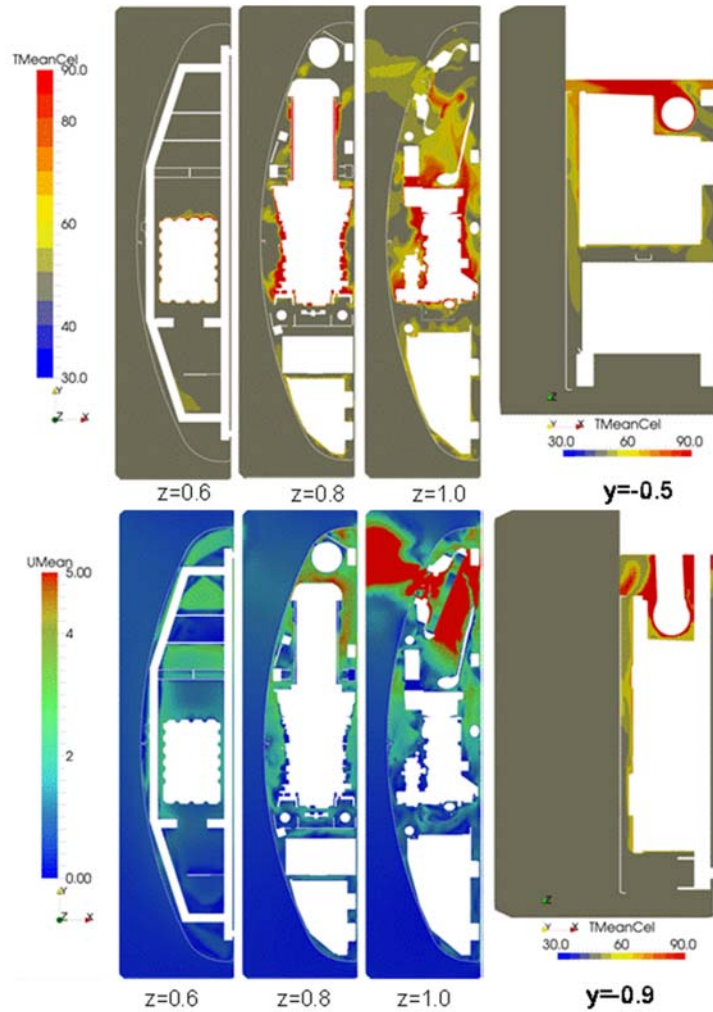


Fig. 11 Cut plots for the summer high-load case at positions $z = 0.6$, $z = 0.8$ and $z = 1.0$ for the temperature and velocity magnitude fields; for the cut planes $y = -0.5$ and $y = -0.9$ the temperature field is shown

IV. CONCLUSION

With the development of the coupled 1D/3D simulation approach, the thermal analysis of transport refrigeration power pack was possible. By studying the summer high-load case, hot areas, such as around the battery, could be identified. The maximum temperatures for the summer high-load case provide an indication of whether further cooling improvements are needed. Through the detailed information about the flow field including the heat fluxes, suggestions for improvement in the cooling design of the power pack unit could be derived directly. For example, it is helpful to direct the flow in such a way, using air baffles for example, that the flow under the fan cannot be sucked in. A possible variant with a baffle is shown in Fig. 12.

Further optimization iterations regarding the design of the power pack unit can now be made directly with the coupled simulation model. An extension of the coupled model to transient thermal scenarios is planned to be able to simulate summer high-load transient scenarios as well. The coupled 1d/3D simulation approach can be easily applied to other applications, such as warm engine compartment flow for electric vehicles.

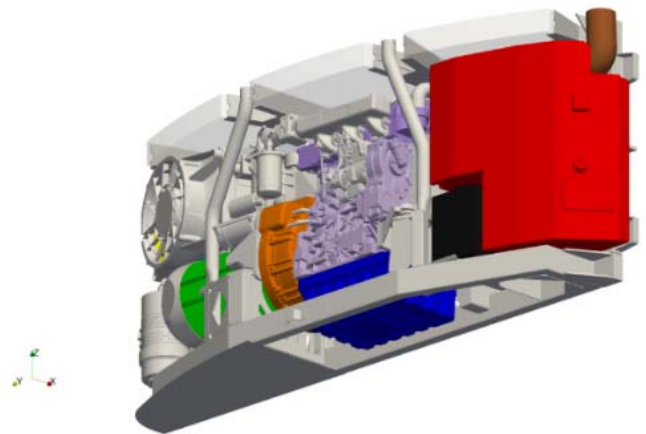


Fig. 12 Possible variant with a baffle to improve the cooling design of the power pack unit

ACKNOWLEDGMENT

The work was partially funded by the Comet K2 – Competence Centers for Excellent Technologies Programme of the Federal Ministry for Transport, Innovation and Technology

(bmvit), the Federal Ministry for Digital, Business and Enterprise (bmdw), the Austrian Research Promotion Agency (FFG), the Province of Styria and the Styrian Business Promotion Agency (SFG).

REFERENCES

- [1] International Energy Agency, 2016. CO₂ emissions from fuel combustion by sector in 2014, in CO₂ Emissions from Fuel Combustion, IEA, 2016. In CO₂ Highlights 2016.
- [2] European Automobile Manufacturers' Association (ACEA), Fact Sheet Trucks. Retrieved July, 20, 2022, from https://www.acea.auto/files/trucks_fact_sheet_ACEA.pdf
- [3] European Federation for Transport and Environment. *Article Road freight emissions*. Retrieved July, 20, 2022, from <https://www.transportenvironment.org/challenges/road-freight/>
- [4] Croquer, S., Benchikh Le Hocine, A.E., & Poncet, S. (2019). Numerical modelling of heat and mass transfer in a refrigerated truck trailer. 25th IIR International Congress of Refrigeration, Montréal, Canada
- [5] Jeong, Jihyuk; Benchikh Le Hocine, Alla Eddine; Croquer, Sergio; Poncet, Sébastien; Bonjour, Jocelyn; and Michel, Benoit, "Numerical Simulation of the Heat Transfer in a Refrigerated Trailer Equipped with Eutectic Plates for Frozen Food Delivery" (2021). International Refrigeration and Air Conditioning Conference. Paper 2253.
- [6] Kospach, A., Bäder, D. Simulation of Engine Compartment Flow with Heat Input. *ATZ Worldw* 121, 36–39 (2019). <https://doi.org/10.1007/s38311-019-0007-5>
- [7] Zhang, C.; Uddin, M.; Robinson, C.; Foster, L. Full vehicle CFD investigations on the influence of front-end configuration on radiator performance and cooling drag. *Applied Thermal Engineering*. 130. 10.1016/j.applthermaleng.2017.11.086.
- [8] Bäder, D.; Kospach, A.; Domaingo, A.: Calculation of air temperatures in the engine compartment of a vehicle. *CFD-Methoden zur Simulation des Wärmeübertragungsverhaltens*, Neuendettelsau, Germany, 2017
- [9] Pengyu Lu, Qing Gao, Yan Wang, "The simulation methods based on 1D/3D collaborative computing for the vehicle integrated thermal management", *Applied Thermal Engineering*, Volume 104, 2016, Pages 42-53, ISSN 1359-4311.
- [10] Yi, H., Li, A., Sun, R., Hu, Y. et al., "1D-3D Coupled Analysis for Motor Thermal Management in an Electric Vehicle," *SAE Technical Paper* 2022-01-0214, 2022, <https://doi.org/10.4271/2022-01-0214>.
- [11] Minovski, B.; Löfdahl, L.; Andrić, J.; Gullberg, P. A Coupled 1D–3D Numerical Method for Buoyancy-Driven Heat Transfer in a Generic Engine Bay. *Energies* 2019, 12, 4156. <https://doi.org/10.3390/en12214156>
- [12] Francesco Fabris, Paolo Artuso, Sergio Marinetti, Silvia Minetto, Antonio Rossetti, "Dynamic modelling of a CO₂ transport refrigeration unit with multiple configurations", *Applied Thermal Engineering*, Volume 189, 2021, 116749, ISSN 1359-4311.
- [13] Kulkarni, C. and Dwyer, H., "Modeling and Performance of Trailer Refrigeration Units with Alternative Power Systems," *SAE Technical Paper* 2007-01-0764, 2007, <https://doi.org/10.4271/2007-01-0764>.
- [14] Barree, R., & M.W., C. (2004). Beyond beta factors: a complete model for Darcy, Forchheimer, and trans-Forchheimer flow in porous media. *SPE Annual Conference and Exhibition*. Houston.
- [15] Moukalled F, Mangani L, Darwish M (2016) *The finite volume method in computational fluid dynamics: an advanced introduction with OpenFOAM® and MATLAB*, volu 113 of Fluid mechanics and its applications. Springer, Cham
- [16] Menter, Florian & Kuntz, M. & Langtry, RB. (2003). Ten years of industrial experience with the SST turbulence model. *Heat and Mass Transfer*. 4.
- [17] W. Sutherland, The viscosity of gases and molecular force, *Philosophical Magazine* 5 (1893), S. 507-531.
- [18] Franzke, R.; Sebben, S.; Bark, T.; Willeson, E.; Broniewicz, A. Evaluation of the Multiple Reference Frame Approach for the Modelling of an Axial Cooling Fan. *Energies* 2019, 12, 2934. <https://doi.org/10.3390/en12152934>